

Blood Flow in Major Cerebral Arteries Measured by Phase-Contrast Cine MR

Dieter R. Enzmann, Michael R. Ross, Michael P. Marks, and Norbert J. Pelc

PURPOSE: To measure mean blood flow in individual cerebral arteries (carotid, basilar, anterior cerebral, middle cerebral, and posterior cerebral) using a cine phase contrast MR pulse sequence. **METHODS:** Ten healthy volunteers (22 to 38 years of age) were studied. The cine phase-contrast section was positioned perpendicular to the vessel of interest using oblique scanning planes. This pulse sequence used a velocity encoding range of 60 to 250 cm/sec. From the velocity and area measurements on the cine images, mean blood flow was calculated in milliliters per minute and milliliters per cardiac cycle. In the same subjects, transcranial Doppler measurements of blood velocity in these same vessels were also obtained. **RESULTS:** There was no difference in blood flow in the paired cerebral arteries. Carotid arteries had mean blood flow in the range of 4.8 ± 0.4 ml/cycle, the basilar artery 2.4 ± 0.2 ml/cycle, the middle cerebral artery 1.8 ± 0.2 ml/cycle, the distal anterior cerebral artery 0.6 ± 0.1 ml/cycle, and the posterior cerebral artery 0.8 ± 0.1 ml/cycle. Overall, there was poor correlation between MR-measured and transcranial Doppler-measured peak velocity. **CONCLUSION:** Although careful attention to technical detail is required, mean blood flow measurements in individual cerebral vessels is feasible using a cine phase-contrast MR pulse sequence.

Index terms: Arteries, carotid; Arteries, cerebral; Arteries, flow dynamics; Arteries, magnetic resonance; Blood, flow dynamics; Blood, magnetic resonance; Magnetic resonance, flow studies

AJNR Am J Neuroradiol 15:123-129, Jan 1994

There has been extensive investigation of cerebral blood flow, with much of this effort directed toward measuring regional cerebral blood flow expressed as milliliters per 100 g of tissue per minute (1-8). Regional cerebral blood flow determination is basic to understanding the pathophysiology of cerebral metabolism and disease processes such as infarction. Less is known about quantitative blood flow in individual cerebral vessels. Volume flow rate has been measured in carotid and basilar arteries in healthy agents and in patients with arteriovenous malformations using a cine phase-contrast (PC) magnetic resonance (MR) technique. Time density curves generated from arteriograms (digital studies), dynamic computed tomography with contrast, and

fast MR scanning with contrast provide qualitative perfusion information, but do not yield quantitative blood flow in individual vessels (9-11). Transcranial Doppler (TCD) provides only blood velocity information in some accessible vessels at the base of the brain (12-14). Development of a quantitative, flow-sensitive MR pulse sequence now permits determination of blood flow in all of the major cerebral vessels of the circle of Willis (15-18). The purpose of this investigation was to demonstrate the technical feasibility of such blood flow measurements using cine PC MR and to determine normal measurements. Such flow measurements would provide valuable quantitative assessment of redistribution of flow in the circle of Willis in stenotic or occlusive cerebrovascular disease.

Received September 2, 1992; accepted pending revision November 19; revision received January 6, 1993.

All authors: Department of Radiology, Stanford (Calif) University School of Medicine. Address reprint requests to Dieter R Enzmann, MD, Department of Radiology, SO72, Stanford University School of Medicine, Stanford, CA 94305-5105.

AJNR 15:123-129, Jan 1994 0195-6108/94/1501-0123

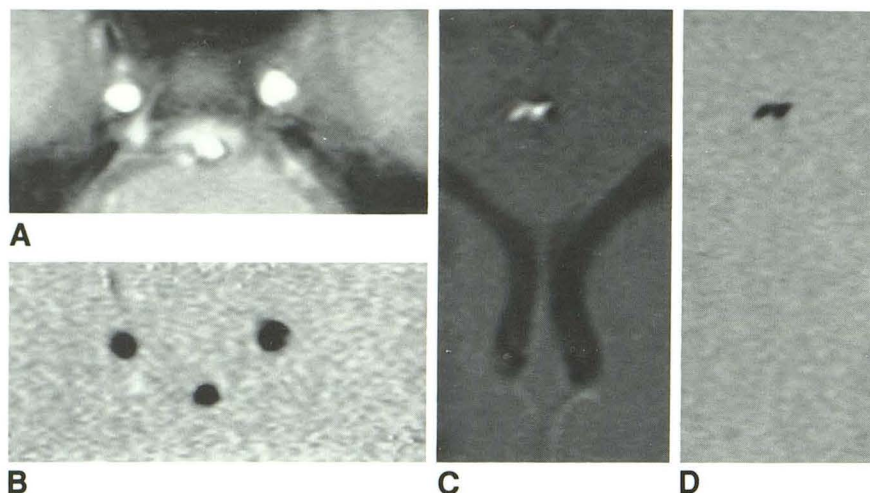
© American Society of Neuroradiology

Materials and Methods

All MR studies were performed on a 1.5-T system (Signa, General Electric, Milwaukee, WI). The cine PC pulse sequence used in this study is one in which the spectrometer cycles at a constant rate (asynchronous to the cardiac

Fig. 1. Axial sections through the carotid and basilar arteries (A, B) and PCalles (C, D).

A, B, Axial magnitude (A) and PC (B) images of both internal carotid arteries (posterior genu of cavernous carotid) and the distal portion of the basilar artery. The PC image (one of 16) depicts these vessels as "black" because of the cephalad direction of blood flow. C, D, Axial magnitude (C) and PC (D) images of the pericallosal arteries as they curve around the genu of the corpus callosum. They are depicted as black throughout the cardiac cycle because of the cephalad direction of blood flow.



cycle) with timing of the phase-encoding increments driven by the cardiac cycle trigger (16). Two interleaved sequences interrogate the same section but with different flow sensitivity at multiple times within each cardiac cycle. The differential flow encoding consists of different first moments of the magnetic field gradient in the slice-select direction. In this investigation the read-out gradient waveform was first-order flow compensated. Differential phase shifts in the two sequences are caused by flow in the slice-select direction. The set of sequences is repeated with the same phase-encoding throughout one cardiac cycle. On detection of a cardiac trigger, the phase-encoding value is incremented. The peripheral pulse was used as the trigger. Because of interference effects of the pulse gradients on the electrocardiogram signal, an electrocardiogram trigger could not be used with the chosen scanning parameters. The imaging time can be as short as 128 cardiac periods (256×128 , number of signals averaged (NSA) = 1), but we used 256×128 and NSA = 2. For a sequence time of 40 msec and single-plane acquisition, the temporal resolution is approximately 80 msec because the two flow encodings are interleaved.

The sensitivity to flow is selectable and parameterized by the velocity, V_{enc} , which produces a differential phase shift of 180° . A V_{enc} of 250 cm/sec was used for the following arteries: carotid, basilar, A1 segment of anterior cerebral artery (ACA), pericallosal artery (PCall), and middle cerebral artery (MCA). A V_{enc} of 60 was used for the posterior cerebral arteries (PCA). Choosing low V_{enc} values improves precision, but potential errors appear because velocities greater than V_{enc} in absolute value are aliased, have an error that is a multiple of $2 V_{enc}$, and appear erroneously inside the $\pm V_{enc}$ range. This flow aliasing is readily recognized because, when it occurs, adjacent pixels have very different velocities (sharp transitions from black to white). Every flow image was viewed to ensure that this error did not occur.

This cine PC MR technique is quantitative without needing calibration, as has been shown in vitro and in vivo (19–21). The sequence generated 16 flow encoded images per cardiac cycle. A region of interest was manually drawn to

encompass the lumen of each of the above vessels. This was performed on the velocity image where the vessels (black or white circles) were easily differentiated from background. If the vessel was oblique in the imaging plane, the magnitude image was used to describe the region of interest to reduce the partial volume effect. The magnitude images were windowed so that the window level was one-half of maximum, window width was 1. The region of interest analysis yielded an average velocity for each of the 16 images, thus providing a velocity profile for the entire cardiac cycle. The zero velocity pixel value was obtained from a large area of brain adjacent to the vessel of interest. Because the brain has no net motion over the cardiac cycle, the average velocity of such an area is zero. Total net blood flow was calculated by multiplying the mean velocity times the area of the vessel lumen (ie, the region of interest). The smallest vessel areas were in the PCall but at least 10 pixels were included in the measurement. A blood flow measurement for each of the 16 images was calculated; mean blood flow was the average of these 16 blood flow data points. The resulting blood flow calculation was expressed in milliliters per minute and milliliters per cardiac cycle. Peak flow (maximum flow in 1 of the 16 images) and peak velocity during the cardiac cycle were also recorded.

Ten healthy volunteers (22 to 38 years old) were studied as follows. A sagittal T1-weighted sequence was the initial scan. From this scan, two axial sections were chosen so that one depicted both carotid arteries at the level of posterior genu in the parasellar region and the distal basilar artery (Fig 1). A second axial section was obtained perpendicular to the pericallosal arteries as they course around the genu of the corpus callosum. A three-dimensional localizing scan using a radio frequency spoiled gradient-echo pulse sequence (30/6/1 [repetition time/echo time/excitations], flip angle = 30° , 256×256 , section thickness = 5 mm) depicted cerebral vessels as bright structures and was used to prescribe the imaging planes graphically. From the three-dimensional spoiled gradient-echo sequence, oblique sagittal scans were positioned perpendicular through the proximal M1 segment of each MCA (Fig 2). Oblique sagittal scans were obtained through the A1 seg-

ments of the ACAs on each side (Fig 3). The PCAs were studied with a single coronal scan positioned so that both PCAs as they encircle the mesencephalon were perpendicular to the imaging plane (Fig 4). The following parameters were used for the phase-contrast cine MR sequence: 40/12/2, flip angle = 30°, matrix 256 × 128, and field of view = 12; the voxel size was 0.47 × 0.94 × 5 mm.

A dedicated TCD unit (Transpect, Medasonics) using a 2-MHz transducer was used for measurements in all of the same subjects. The middle and anterior cerebral arteries were examined via the transtemporal window with a handheld technique. This window is usually found 1 to 3 cm above the zygomatic arch. This approach minimized acoustic scatter caused by the relative absence of sound attenuating diploic trabeculations in the thin squamosal portion of the temporal bone.

The middle, anterior, and posterior cerebral arteries were identified by their direction of flow, their depth or distance from the temporal bone, and their relationship to the terminal portion of the supraclinoid carotid artery. Both audible and visual display features allow the operator to determine whether the Doppler signal is moving toward or away from the transducer. With the probe positioned at the temporal window, flow toward the transducer indicates signal from the middle and posterior cerebral artery and flow away from the transducer denotes the anterior cerebral artery.

The M1 segment of the MCA is identified as a Doppler signal flowing toward the transducer at a depth of 45 to 55 mm. The depth-stepping feature of the machine allows progressively deeper focusing of the sound beam until a reversal of flow direction is detected. Upon traversing the

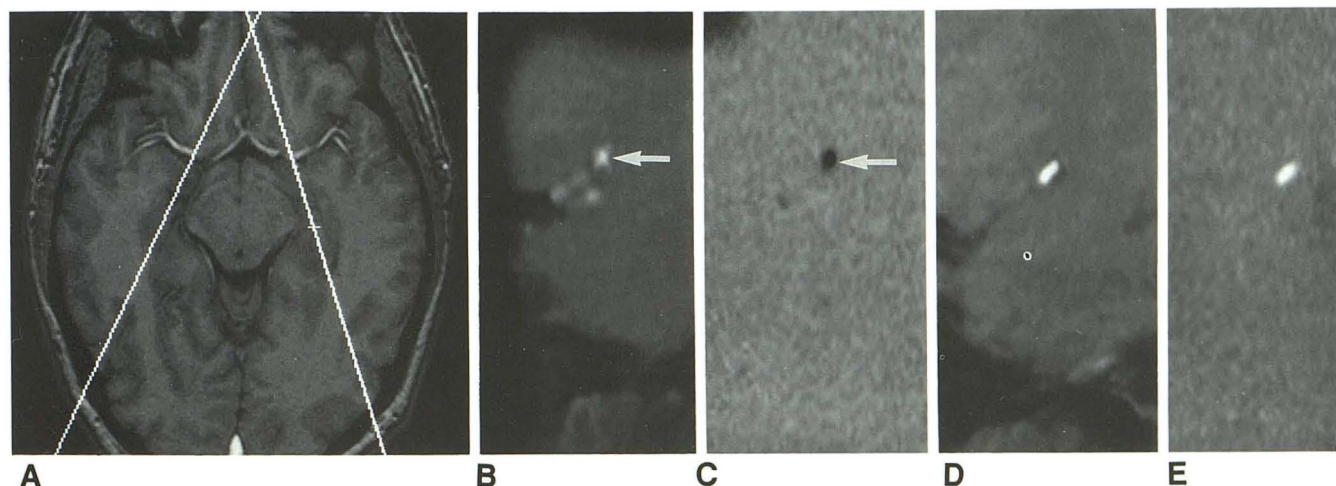


Fig. 2. A, Axial spoiled gradient-echo image through the MCA showing the sagittal plane selection for the cine MR sequence so that the imaging plane for this flow sequence is perpendicular to the MCA.

B, C, Sagittal oblique magnitude (B) and PC (C) images through the proximal, horizontal portion of the right MCA (arrows, B, C). The PC image is one of 16, all of which showed the middle cerebral artery to be of black intensity, indicating continuous flow toward the right throughout the cardiac cycle. D, E, Oblique, sagittal magnitude (D) and PC (E) images of the proximal horizontal portion of the left middle cerebral artery. The PC image (E) is one of 16 depicting the left MCA as white intensity throughout the cardiac cycle. Because of the slight obliquity to the MCA, the magnitude image was used for determining the region of interest.

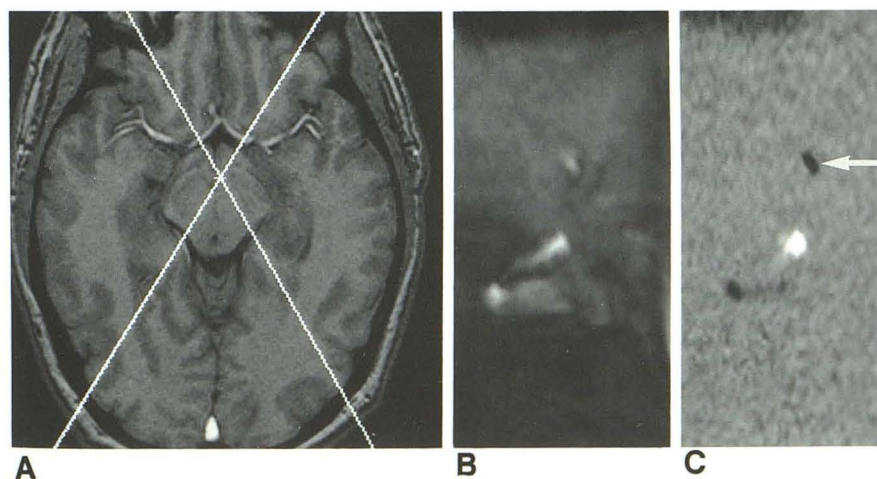


Fig. 3. A, Same axial spoiled gradient-echo images as in Figure 2 but now used to position oblique sagittal planes so they are perpendicular to the A1 segments of each anterior cerebral artery.

B, C, Oblique sagittal magnitude (B) and PC (C) image of the left A1 segment. The PC image (one of 16) showed the left A1 segment (arrow) depicted as "black," indicating flow toward the right. The bright signal below the A1 segment is the supraclinoid carotid artery with flow toward the left, ie, "white" intensity.

Fig. 4. A, Axial spoiled gradient-echo image at the level of the midbrain shows orientation of the coronal plane perpendicular to both posterior cerebral arteries as they circumvent the mesencephalon.

B, C, The coronal magnitude (B) and PC (C) images of both PCAs. With flow encoding in the anteroposterior direction, the posterior cerebral arteries are depicted as "white" intensity throughout the cardiac cycle.

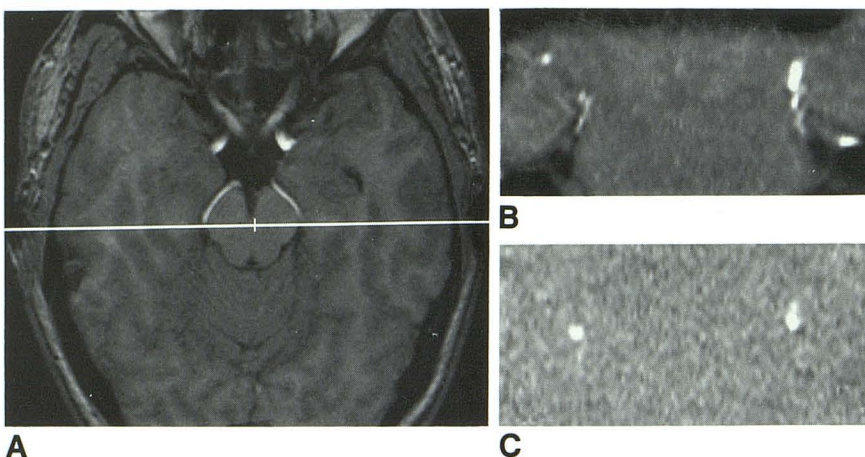


TABLE 1: Mean \pm SE of the mean blood flow measurements determined by the cine MR technique and peak blood flow as determined from the 16 images

	Blood Flow (ml/min)						Blood Flow (ml/cycle)			
	Right			Left			Right		Left	
	Mean	Peak	Vessel Area (cm ²)	Mean	Peak	Vessel Area (cm ²)	Mean	Peak	Mean	Peak
Carotid	302 \pm 21	389 \pm 28	0.22 \pm 0.06	337 \pm 19	440 \pm 31	0.22 \pm 0.06	4.6 \pm 0.4	5.9 \pm 0.5	5.1 \pm 0.3	6.6 \pm 0.5
A1-ACA	88 \pm 11	105 \pm 13	0.10 \pm 0.04	75 \pm 10	91 \pm 11	0.09 \pm 0.04	1.3 \pm 0.2	1.6 \pm 0.2	1.1 \pm 0.2	1.4 \pm 0.2
PCALL	44 \pm 5	52 \pm 6	0.06 \pm 0.02	42 \pm 5	48 \pm 6	0.06 \pm 0.02	0.6 \pm 0.1	0.7 \pm 0.1	0.6 \pm 0.1	0.7 \pm 0.1
MCA	127 \pm 7	152 \pm 10	0.15 \pm 0.04	108 \pm 7	126 \pm 8	0.13 \pm 0.04	1.8 \pm 0.2	2.1 \pm 0.3	1.7 \pm 0.1	1.9 \pm 0.2
PCA	51 \pm 4	64 \pm 5	0.09 \pm 0.3	53 \pm 4	68 \pm 5	0.09 \pm 0.04	0.8 \pm 0.1	0.9 \pm 0.1	0.8 \pm 0.1	1.0 \pm 0.1
Basilar	161 \pm 11	203 \pm 13	0.14 \pm 0.03				2.4 \pm 0.2	3.1 \pm 0.2		

Note: PCALL = pericallosal artery; MCA = middle cerebral artery; PCA = posterior cerebral arteries.

terminal portion of the carotid siphon, the A1 segment of the anterior cerebral artery is detected as flow away from the transducer at a depth of 55 to 65 mm. From this point, posterior angulation exhibits the PCA as flow toward the transducer. Insonation of the basilar artery is achieved by placing the transducer midline at the foramen magnum and directing the beam parallel to the sagittal plane at a depth of 60 to 70 mm. Flow should be away from the transducer. After these vessels were satisfactorily identified, printed recordings were obtained of the waveform and of the peak and mean systolic velocities.

Statistical analysis used a two-tailed Student *t* test for comparison of mean blood flow measurements. A correlation coefficient was calculated to compare MR and TCD blood velocity measurements.

Results

Net mean blood flow (mean \pm standard error of the mean) is expressed in two ways: milliliters per minute and milliliters per cardiac cycle. The latter number controls for differences in heart rate between subjects in that it represents mean blood flow per cardiac period. There was no significant difference in mean blood flow between the right and left sides for any of the paired

cerebral vessels (Table 1). This was true for volume blood flow per minute and per cardiac cycle. Mean basilar artery flow was approximately 25% of total carotid flow for both measurements. Peak blood flow rates in the carotid and basilar arteries were in the range of 26% to 31% above the mean blood flow rate.

The MCA showed the right MCA to have a mean blood flow slightly higher than the left MCA but this was not statistically significant ($P = .10$). Peak MCA blood flow during the cardiac cycle was 25% to 28% above the mean flow rate. A comparison of the flow profile in the MCA, carotid, and basilar arteries is shown in Figure 5.

The ACA was studied in two locations: the A1 segment (A1-ACA) and the PCall at the genu of the corpus callosum. There was no significant difference in blood flow between the right and left A1-ACAs, although there was greater variability in those measurements compared with the other cerebral vessels (Table 1). Peak flow rate was 21% above the mean blood flow rate. Blood flow in the more distal PCall was lower and peak

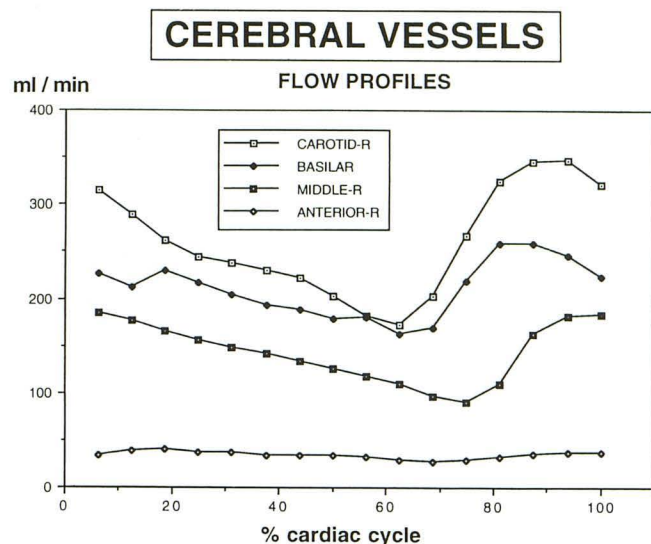


Fig. 5. Flow profiles during the cardiac cycle are shown for the right carotid artery, right MCA, right anterior cerebral artery (PCall), and basilar artery of a single individual. Note the prominent pulse waves in the carotid, basilar, and MCA compared with the PCall. Although the systolic upstroke is nearly simultaneous in the carotid and basilar arteries, peak flow occurs earlier in the basilar artery compared with the carotid artery. Basilar peak flow is earlier by approximately 12% of the cardiac cycle. Peak flow in the MCA is delayed by approximately 12% of the cardiac cycle compared with the carotid artery and approximately 25% of the cycle compared with the basilar artery. Blood flow is expressed in milliliters per minute.

flow was also 21% to 23% above the mean blood flow rate.

Mean PCA flow was symmetric (Tables 1 and 2) with peak flow 25% to 28% above the mean blood flow rate (Table 1). Pulsatility in both the PCall and PCAs was less compared with carotid, basilar, and MCAs (Fig 5).

Peak blood flow in each of the vessels during the cardiac cycle is shown in Table 1. These peak flows were in the range of 21% to 31% higher than the mean blood flow in the individual vessels. Systole showed an upswing in blood flow in all the vessels. This was delayed in the MCA compared with the basilar and carotid arteries. Peak blood flow in the MCA was approximately 12% of the cardiac cycle behind the carotid and basilar peak. There was a slow decline of blood flow during diastole. The mean of peak blood velocities as determined by MR fell into a broad range of 53 to 62 cm/sec for the following vessels: carotid, basilar, A1-ACA, and MCA. The PCalls and PCA fell into a lower peak velocity range, 27 to 31 cm/sec (Table 2).

TCD was used to measure mean and peak blood velocity in each of the above arteries except

the PCall. The overall correlation between TCD and MR peak velocities was poor ($r = .435$). The MCA velocities correlated poorly (MR peak vs TCD peak, $r = .200$). The right-to-left comparison of MR peak, TCD peak, and TCD mean velocities showed no significant differences. In general, peak MR velocity measurements were lower than TCD peak velocities.

Discussion

A number of techniques have been used to determine quantitatively regional cerebral blood flow (1–8). This determination of blood flow is important for assessing tissue metabolism and viability. The cerebral blood flow measurements obtained with the cine PC method provide different and complementary information. There currently is no standard for measuring blood flow in individual cerebral arteries. There is no method of validating the accuracy of these cerebral blood flow measurements in vivo and, thus, flow phantom measurements and in vivo measurements in other vessels are the foundation for presumed accuracy (19–21). This cine PC MR technique of measuring flow has been shown to be accurate in in vitro testing using constant velocity and pulsatile flow (19, 21). An in vivo experiment in noncerebral vasculature has shown high accuracy for this MR technique (20). The potential errors in blood flow measurement using the cine PC MR technique also have been analyzed (22). This investigation measured net blood flow in cerebral vessels, where flow is antegrade throughout the cardiac cycle, so blood flow measurement errors would be expected to be less than in vessels such as the ascending aorta, where reverse flow occurs in the cardiac cycle (22). The potential problem of partial volume error was addressed by imaging perpendicular to the vessel of interest using oblique scanning planes. When this was not achieved, using the appropriate windowing on the magnitude image reduces the partial volume error (see Methods) (20). The number of pixels per vessel area was maximized using a small field of view. The velocity-encoding range was matched to the expected velocities in the vessel of interest; this was based on previous pilot data. This range was chosen to avoid aliasing and was kept constant throughout the cardiac cycle (22). The V_{enc} values chosen for each of the cerebral vessels were based empirically on our previous study and subsequent pilot work. We increased the V_{enc} in the carotid compared with previous studies (18)

TABLE 2: Mean \pm SE of the mean of blood velocity in each of the major cerebral vessels as determined by cine MR and transcranial Doppler (TCD)

	Blood Velocity (cm/sec)					
	MR Peak		TCD Peak		TCD Mean	
	Right	Left	Right	Left	Right	Left
Carotid	51 \pm 3	43 \pm 4	69 \pm 4	72 \pm 5	40 \pm 3	43 \pm 4
A1-ACA	52 \pm 11	44 \pm 6	77 \pm 3	86 \pm 5	50 \pm 2	53 \pm 3
PCALL	30 \pm 2	31 \pm 2				
MCA	62 \pm 5	47 \pm 5	96 \pm 4	100 \pm 5	61 \pm 2	65 \pm 3
PCA	29 \pm 2	27 \pm 1	60 \pm 3	62 \pm 4	38 \pm 2	40 \pm 3
Basilar	56 \pm 5		52 \pm 3		36 \pm 2	

Note: Abbreviations are as in Table 1.

because in healthy people aliasing could be detected at the posterior genu of the cavernous internal carotid artery at $V_{enc} = 150$ cm/sec. Although the V_{enc} appears low for the PCA, we have not detected aliasing at the value of 60 cm/sec.

Cine PC MR has been used previously to measure flow in the carotid and basilar arteries (18), and there has been one report of its use in measuring blood flow in the middle cerebral artery (Tarnawski, Society of Magnetic Resonance in Medicine, 1989). The mean blood flow for the right ($121.7 \pm 3.8\%$) and left ($106.1 \pm 4.1\%$) MCAs in that abstract compare closely with our values of 127 ± 7 ml/min and 108 ± 7 ml/min for the right and left MCAs, respectively. Blood flow measurements in the carotid and basilar arteries in this investigation of healthy volunteers are very similar to measurements made in a previous study of healthy volunteers and patients (18). If blood flow in the proximal anterior, middle, and posterior cerebral arteries are summed then the MCA distribution receives approximately 46% of this total blood flow, the anterior cerebral circulation receives 34%, and the PCAs receive 20%. Peak blood flow in systole was 20% to 30% higher than mean blood flow for all the individual cerebral vessels.

The blood velocity measurements of the cine PC technique and those of TCD differed. TCD peak velocity measurements were approximately 30% to 40% higher than peak cine PC measurements. These differences in peak velocity were consistent and nearly proportional for each cerebral artery. A difference in peak velocity was not unexpected. With the cine PC technique, the actual peak velocity in a parabolic flow profile would be underestimated because of averaging within the voxel, averaging over hundreds of cardiac cycles, and because of the more limited

temporal resolution. TCD has better temporal resolution than the cine PC technique used in this study, resulting in less temporal averaging, which would raise the peak. To the extent that plethysmographic gating is less precise than electrocardiogram gating, our temporal resolution suffered further. TCD peak velocity is not a mean but the instantaneous peak in one cardiac cycle. For the TCD measurement the volume of interrogation is not known but, presumably, it is smaller than with MR. This would result in a higher peak velocity; that is, less averaging than with the MR method. Because the angle of interrogation is not measurable with TCD, deviation from the perpendicular MR measurement would be expected. Because the angle is not known, corrections are not easily calculated. This error, however, would tend to underestimate the velocity. In addition, the location of the measurement in the vessel of interest likely differed between MR and TCD; the latter location was less accurately identified.

Although a comparison of blood velocity measurements by the MR and TCD techniques was interesting, a close correlation was not expected because of the above-enumerated differences in these two techniques. This comparison was carried out with the expectation that there would be differences between the two techniques and that, in fact, these two methods provide different information. Because the purpose of the MR examination is to measure volume blood flow, the TCD study is not really a competitive examination. TCD blood velocity measurements are not used for the calculation of volume blood flow but are generally used in the clinical setting as an early indicator of the onset of vasospasm with the patient serving as his or her own control. The cine MR technique is unlikely to be used in this setting because TCD is a bedside examination.

The regional cerebral blood flow measurements help to explain and delineate tissue viability in the spectrum of cerebral ischemic diseases. These measurements of tissue blood flow are valuable because they take into account all forms of collateral flow. What regional cerebral blood flow measurements do not define are the routes and magnitude of collateral blood flow. How blood flow is redistributed in the circle of Willis cannot be determined from regional cerebral blood flow studies. The cine PC technique has the ability to depict how and to what extent blood flow is redistributed in the circle of Willis in either high-flow or low-flow states (17). In low-flow states, such as carotid stenosis or occlusion, blood flow measurements in cerebral arteries can indicate the source of collateral blood flow and its relative quantitative importance. The redistribution of blood could, therefore, be measured in patients with atherosclerotic disease to determine the significance of a stenotic or occlusive lesion. The importance of a collateral supply could also be tested by performing the cine PC blood flow study before and after a carbon dioxide or Diamox challenge. In a similar fashion, the increased blood flow in arteriovenous malformation feeding vessels could be measured (18). The cine PC technique provides a method for investigating the blood flow distribution in vessels of the circle of Willis and the response to various interventions.

References

- Giller C, Purdy P, Lindstrom WW. Effects of inhaled stable Xenon on cerebral blood flow velocity. *AJNR: Am J Neuroradiol* 1990;11:177-182
- Gur D, Wolfson SK, Yonas H. Progress in cerebrovascular disease: local cerebral blood flow by Xenon enhanced CT. *Stroke* 1982;13:750-758
- Gur D, Yonas H, Jackson DL, et al. Simultaneous measurement of cerebral blood flow by the Xenon/CT method and the microsphere method. *Invest Radiol* 1985;20:672-677
- Holman BL, Hill TC, Magistretti PL. Brain imaging with emission computed tomography and radiolabeled amines. *Invest Radiol* 1982;17:206-215
- Ito M, Lammertsma AA, Wise RJ, et al. Measurement of regional cerebral blood flow and oxygen utilisation in patients with cerebral tumours using ^{15}O and positron emission tomography: analytical techniques and preliminary results. *Neuroradiology* 1982;23:63-74
- Norrving B, Nilsson B, Risberg J. rCBF in patients with carotid occlusion. Resting and hypercapnic flow related to collateral pattern. *Stroke* 1982;13:155-162
- Uemura K, Kanno I, Miura Y. Tomographic study of regional cerebral blood flow in ischemic cerebrovascular disease by $^{81\text{m}}\text{Kr}$ intraarterial infusion and Headtome. *J Comput Assist Tomogr* 1982;6:677
- Yonas H, Wolfson SK, Gur D, et al. Clinical experience with the use of Xenon-enhanced CT blood flow mapping in cerebral vascular disease. *Stroke* 1984;15:443-450
- Traupe H, Heiss WD, Hoeffken W, Zölch. Perfusion patterns in CT transit studies. *Neuroradiology* 1980;19:181-191
- Norman D, Axel L, Berninger WH, et al. Dynamic computed tomography of the brain: techniques, data analysis, and applications. *AJNR: Am J Neuroradiol* 1981;2:1-12
- Berninger WH, Axel L, Norman D, Napel S, Redington RW. Functional imaging of the brain using computed tomography. *Radiology* 1981;138:711-716
- Aaslid R. Transcranial doppler examination techniques. In: Aaslid R, ed. *Transcranial Doppler sonography*. New York: Springer-Verlag, 1993:39-59
- Aaslid R, Huber P, Nornes H. A transcranial doppler method in the evaluation of cerebrovascular spasm. *Neuroradiology* 1986;28:11-16
- Mattle H, Grolimund P, Huber P, Sturzenegger M, Zurbrugg HR. Transcranial doppler sonographic findings in middle cerebral artery disease. *Arch Neurol* 1988;45:289-295
- Nayler GL, Firmin DN, Longmore DB. Blood flow imaging by cine magnetic resonance. *J Comput Assist Tomogr* 1986;10:5
- Pelc JN, Herfkens RJ, Shimakawa A, Enzmann DR. Phase contrast cine magnetic resonance imaging. *Magn Reson Q* 1991;7:229-254
- Ross MR, Pelc NJ, Enzmann DR. Qualitative phase contrast MR angiography in the normal and abnormal circle of Willis. *AJNR Am J Neuroradiol* 1993;14:19-25
- Marks MP, Pelc NJ, Ross MR, Enzmann DR. Determination of cerebral blood flow with a phase-contrast cine MR imaging technique: evaluation of normal subjects and patients with arteriovenous malformations. *Radiology* 1992;182:467-476
- Spritzer CE, Pelc NJ, Lee JN, Evans A, Sostman HD, Riederer SJ. Preliminary experience with rapid MR blood flow imaging using a phase sensitive limited flip angle gradient refocused pulse sequence. *Radiology* 1990;176:255-262
- Pelc LR, Pelc NJ, Rayhill SC, et al. Arterial and venous blood flow: noninvasive quantitation with MR imaging. *Radiology* 1992;185:809-812
- Evans AJ, Iwai F, Grist TA, et al. MR imaging of blood flow with a phase subtraction technique: in vitro and in vivo validation. *Invest Radiol* 1993;28:109-115
- Buoncore MH, Bogren H. Factors influencing the accuracy and precision of velocity-encoded phase imaging. *Magn Reson Med* 1992;26:141-154